



# Soil erosion as transport pathway of microplastic from agriculture soils to aquatic ecosystems



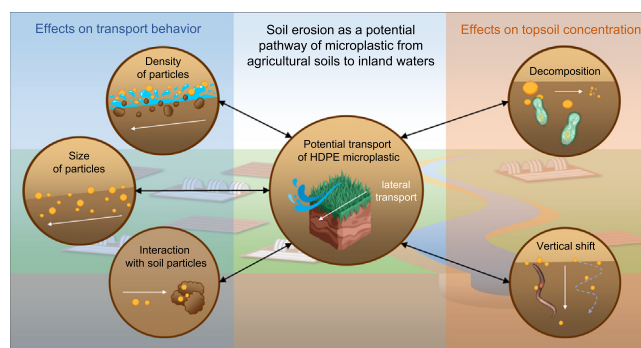
Raphael Rehm, Tabea Zeyer, Arthur Schmidt, Peter Fiener \*

University of Augsburg, Institute of Geography, Alter Postweg 118, 86159 Augsburg, Germany

## HIGHLIGHTS

- Coarse HDPE-MP is preferentially eroded and hence enriched in delivered sediments
- HDPE-MP erosion decreases over time due to increasing soil-MP interactions
- Lateral HDPE-MP fluxes increase and vertical fluxes decrease with MP particle size

## GRAPHICAL ABSTRACT



## ARTICLE INFO

### Article history:

Received 5 March 2021

Received in revised form 4 June 2021

Accepted 27 June 2021

Available online 6 July 2021

Editor: Manuel Estaban Lucas-Borja

### Keywords:

Microplastic  
Plasticulture  
Aggregation  
Soil erosion  
HDPE

## ABSTRACT

Soil erosion is a potentially important source of microplastic (MP) entering aquatic ecosystems. However, little is known regarding the erosion and transport processes of MP from agricultural topsoils. The aim of this study is to analyze the erosion and transport behavior of MP during heavy rainfall events, whereas a specific focus is set to preferential MP transport and MP-soil interactions potentially leading to a more conservative transport behavior. The study is based on a series of rainfall simulations on paired-plots ( $4.5 \text{ m} \times 1.6 \text{ m}$ ) of silty loam and loamy sand located in Southern Germany. The simulations (rainfall intensity  $60 \text{ mm h}^{-1}$ ) were repeated 3 times within 1.5 years. An amount of  $10 \text{ g m}^{-2}$  of fine ( $\text{MP}_f$ , size  $53\text{--}100 \mu\text{m}$ ) and  $50 \text{ g m}^{-2}$  of coarse ( $\text{MP}_c$ , size  $250\text{--}300 \mu\text{m}$ ) high-density polyethylene as common polymer was added to the topsoil ( $<10 \text{ cm}$ ) of the plots. The experiments show a preferential erosion and transport of the MP leading to a mean enrichment ratio of  $3.95 \pm 3.71$  ( $\text{MP}_c$ ) and  $3.17 \pm 2.58$  ( $\text{MP}_f$ ) in the eroded sediment. There was a higher MP enrichment on the loamy sand but a higher sediment delivery on the silty loam resulting in nearly equal MP deliveries from both soil types. An increasing interaction with mineral soil particles or aggregates leads to a decreasing MP delivery over time. Within 1.5 years, up to 64% of the eroded MP particles were bound to soil particles. Overall, more of the  $\text{MP}_c$  was laterally lost via soil erosion, while for the  $\text{MP}_f$  the vertical transport below the plough layer was more important. In general, our study indicates that arable land susceptible to soil erosion can be a substantial MP source for aquatic ecosystems.

© 2021 The Authors. Published by Elsevier B.V. This is an open access article under the CC BY license (<http://creativecommons.org/licenses/by/4.0/>).

## 1. Introduction

In the Anthropocene, plastic has replaced many traditional materials such as wood, glass and metal. The diverse properties of plastics and low

production costs, explain the strong dominance of this material. However, longevity of plastic also poses a threat to our environment (Ng et al., 2018). Since conventional synthetic plastic is hardly biodegradable and larger particles slowly decay into micro- (MP) and nanoplastic, small particles accumulate in all environmental systems (Gasperi et al., 2018; Horton et al., 2017; Saling et al., 2020). As a result, plastic waste has become a major environmental issue of our time and

\* Corresponding author.

E-mail address: [peter.fiener@geo.uni-augsburg.de](mailto:peter.fiener@geo.uni-augsburg.de) (P. Fiener).

there is growing concern of global MP pollution (Lambert and Wagner, 2018; Tagg and do Sul, 2019; Xu et al., 2020). Most MP studies focus on oceans (Ajith et al., 2020; Liu et al., 2020; Saling et al., 2020), beach sediments (Coppock et al., 2017; Li et al., 2019; Stolte et al., 2015) and inland waters (Besseling et al., 2017; Koelmans et al., 2019; Lambert and Wagner, 2018); and the results have received wide public attention. In comparison terrestrial systems, especially soils, are still understudied (Blasing and Amelung, 2018; Rillig and Bonkowski, 2018; Zhou et al., 2020). However, soil contamination should be treated with the same global concern as marine and freshwater ecosystems, since arable soils alone are likely to contain more MP than the oceans (de Souza Machado et al., 2018; Nizzetto et al., 2016b; Rillig and Lehmann, 2020). Arable soils can be polluted with MP via several pathways. On the one hand side MP is entering agricultural soils with intentionally used soil amendments, e.g. sewage sludge (Corradini et al., 2019; van den Berg et al., 2020), compost (Braun et al., 2020) and digested residues (Weithmann et al., 2018) or via tire wear (Baensch-Baltruschat et al., 2020) and atmospheric deposition (Dris et al., 2015). On the other hand side MP in agricultural soils results from the decay of plastic materials used in agriculture, such as mulch films (Espí et al., 2016; Qi et al., 2020) or binding material in special crops (Rehm et al., 2018). Despite our general knowledge regarding potential MP sources in agricultural soils, there is not sufficient data of in-situ soil contamination mostly because of the difficulty to detect MP in the soil matrix (da Costa et al., 2019; Li et al., 2020; Moeller et al., 2020). Nevertheless, most estimates based on MP input into soils consider agricultural soils to be a significant MP sink (Rochman, 2018; Waldschläger et al., 2020; Zubris and Richards, 2005). Whether the accumulation of MP in the soil leads to a permanent sink (until the plastic disintegrates after centuries), or is lost again through leaching into the groundwater or through surface runoff and erosion, is often discussed, but it is hardly quantified (Mai et al., 2018; Nizzetto et al., 2016a; Rillig et al., 2017a). Since agricultural soils in particular are affected by erosion, the possible transport of MP via surface runoff is of great interest. Initial studies suggest a significant MP delivery from agricultural soils (Crossman et al., 2020). In the Rhône River, a peak in plastic transport was measured a few days after precipitation events, indicating that surface runoff may have an important effect of MP input to water bodies compared to other processes (Castro-Jiménez et al., 2019).

The major aim of this study is to shed light on the behavior of high density polyethylene (HDPE) MP particles once they have entered the plough layer of agricultural soils if subjected to severe soil erosion. A PE polymer was used in this study as it was identified as the potentially most common plastic type to be expected in arable soils (Koutnik et al., 2021; Huerta Lwanga et al., 2018; Piehl et al., 2018). This study will test the following hypotheses: (i) Due to the comparatively low density of plastic particles, preferred erosion leads to an accumulation of MP in the delivered sediments compared to the parent soil contaminated with MP. (ii) The MP enrichment will increase with decreasing MP size, while overall MP enrichment is more pronounced if the MP is in the same or a smaller size range as the mineral soil particles. (iii) Over time, MP delivery will decrease as MP-soil interactions (aggregation and binding to mineral particles) increase and topsoil MP concentrations will decline due to subsequent erosion events and vertical transport below the plough layer.

## 2. Materials and methods

### 2.1. Experimental design

This study was carried out at two experimental farms representing intensively used arable land in Southern Germany, located in Freising (latitude 48°24'16"; longitude 11°41'42") and Strass (latitude 48°42'28"; longitude 11°03'05"). Both sites show distinctively different soil textures, namely a silty loam (16% sand, 59% silt, 25% clay) with somewhat higher mean topsoil organic carbon contents of 1.3% in Freising

and a loamy sand (72% sand, 18% silt, 10% clay) with lower mean topsoil organic carbon contents of 0.9% in Strass. At both sites, slopes of 3° were chosen, where two paired rainfall simulation plots were installed in August 2018 to study the lateral transport of HDPE particles in a size of 53–100 µm and 250–300 µm. The choice of MP size was based on the fraction sizes of soil micro- and macro-aggregates (see Section 2.5). The plots had a dimension of 1.6 m × 4.5 m and were boarded by metal plates reaching 0.15 m deep into the soil. At the downslope end of the plots a stainless-steel funnel was installed to measure runoff during the experiments (Fig. 1). Next to the plots six stainless-steel cylinders (0.25 m diameter, 0.5 m height) were inserted into the soil for 0.45 m to study vertical movement of the same HDPE microplastic particles (Fig. 1). To investigate whether the MP used in this study degraded during the 1.5-years experimental phase, MP samples of 250–300 µm HDPE were buried in stainless-steel mesh bags (30 mm × 60 mm, 180 µm mesh size) at a depth of 0.05 m.

The plots and the cylinders were spiked with the two different MP size fractions. Commercially available dry milled HDPE (Schaetti AG; Wallisellen, Switzerland) without additives, at a density of 0.975 g cm<sup>-3</sup> and a melting point of 127–135 °C was dry-sieved in the laboratory to obtain a fine MP with a diameter of 53–100 µm (MP<sub>f</sub>) and a coarse MP with a diameter of 250–300 µm (MP<sub>c</sub>) fraction. Especially HDPE particles were used for pragmatic reasons as its production cost are much lower compared to low density polyethylene (LDPE) due to

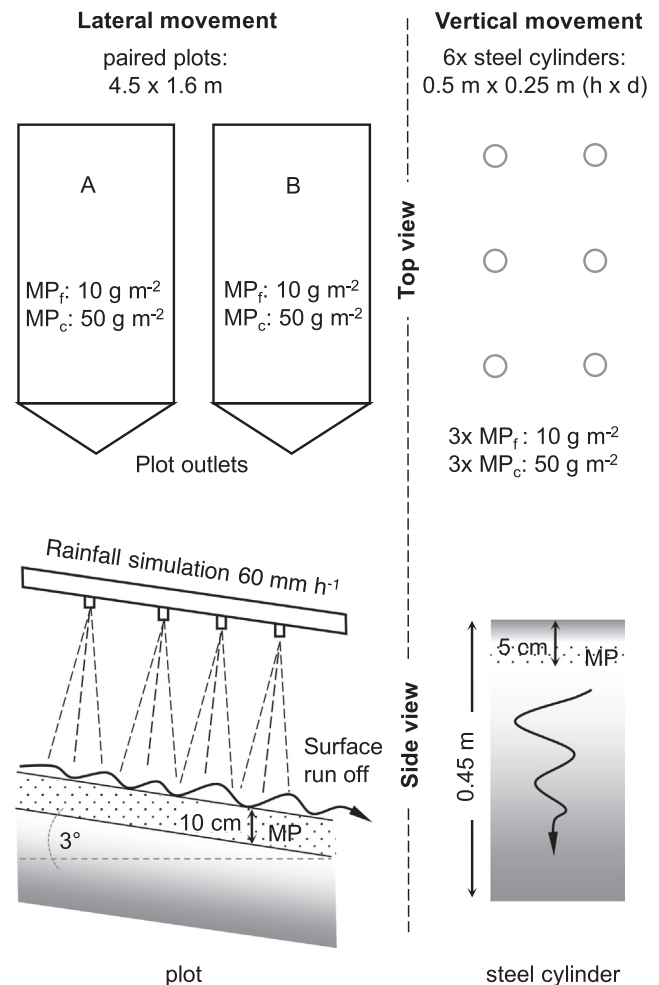


**Fig. 1.** Top and side view of the set up in the field for a 1.5 years experiment for lateral (left side) and vertical (right side) high density polyethylene (HDPE) microplastic (MP) movement observation. For lateral movement, MP (MP<sub>f</sub> is fine MP, 53–100 µm; MP<sub>c</sub> is coarse MP, 250–300 µm) was added to the topsoil of paired plots (A and B) and treated with a series of rainfall simulations. For vertical movement, stainless-steel cylinders were inserted into the soil to study the vertical movement of MP.

easier milling procedures. The size distribution within each MP fraction was determined using a digital microscope (Keyence VHX 6000, Japan) and proofed for normal distribution using QQ-plots.

At the beginning of the experimental phase,  $10 \text{ g m}^{-2}$  of  $\text{MP}_f$  and  $50 \text{ g m}^{-2}$  of  $\text{MP}_c$  was added to all plots. Due to the known properties of the MP, this corresponds to  $1.02 \cdot 10^9$  ( $\text{MP}_f$ ) and  $40.7 \cdot 10^6$  ( $\text{MP}_c$ ) particles added per plot (Fig. 1). To ensure spatial homogeneity within the plots, the same amount of MP was added per  $\text{m}^2$  on the surface using a fine meshed kitchen strainer. After surface application the MP was mixed into the upper 10 cm of topsoil by ploughing using an electric garden hoe (Hecht 745; Hecht; Germany) followed by a 30 kg lawn roller (Hecht 501; Hecht; Germany). The topsoil of the stainless-steel cylinders was loaded with the same MP concentrations. In contrast to the plots, the upper 5 cm of the topsoil was removed, MP was mixed into the 3–5 cm layer and covered by 2 cm of MP free topsoil, to avoid potential MP loss via splash or wind erosion (Fig. 1). At each study site, three of six cylinders were loaded with  $\text{MP}_f$  and the other three cylinders were loaded with  $\text{MP}_c$ . The stainless-steel mesh bags nets were filled with 0.2 g of  $\text{MP}_c$  only.

The topsoil of the plots were loaded with a relatively high MP concentration ( $\text{MP}_f$ : about 77 mg or  $1.1 \cdot 10^6$  particles  $\text{kg}^{-1}$  soil;  $\text{MP}_c$ : about 385 mg or  $4.35 \cdot 10^4$  particles  $\text{kg}^{-1}$  soil) for three reasons: (i) Adding MP was only done at the beginning of the experimental period to determine changes in erosion and transport behavior over time. As such, the MP concentrations needed to be high enough to ensure that even after a series of rainfall simulations and a potential loss below the plough layer a substantial amount of MP was left in topsoil. (ii) The added concentrations were also high enough to avoid potential bias via minimal background concentrations. (iii) The concentrations needed to be above the detection limit of the used MP measurements (see Section 2.7). Even if the used MP concentrations are relatively high, similar concentrations are documented in heavily contaminated soils, e.g. Vollertsen and Hansen (2017) found concentrations up to  $2.4 \cdot 10^5$  MP (10–500  $\mu\text{m}$ ) particles  $\text{kg}^{-1}$  soil in farmland soils in Denmark.

## 2.2. Rainfall simulation – lateral MP fluxes

The rainfall simulation (RS) was carried out with a 'Weihestephaner Schwenkdüsenregner' after Kainz and Eicher (1991). The rainfall simulator works with four swivelling nozzles (Veejet 80/100) producing a median drop diameter of 1.9 mm, a mean ( $\pm$  standard deviation) kinetic energy of  $19.1 \pm 2.3 \text{ J m}^{-2} \text{ mm}^{-1}$  rain and a mean drop falling velocity of  $6.8 \pm 0.82 \text{ m s}^{-1}$  (Auerswald et al., 1992; Kainz et al., 1992). In four test runs the rainfall simulator was calibrated to reach a near constant rainfall intensity of  $60.9 \pm 5.28 \text{ mm h}^{-1}$ , while spatial homogeneous rainfall coverage of the plot area was shown using 96 cups placed in a  $0.3 \text{ m} \times 0.3 \text{ m}$  grid (mean coefficient of variation within the plot for four simulations: 8.66%).

At both test sites, three series of rainfall simulations were carried out in August 2018 (RS1), July 2019 (RS2) and November 2019 (RS3). One RS consisted of a sequence of two 30-min runs (rainfall intensity  $60.9 \text{ mm h}^{-1}$ ) with a gap of 30 min in between to simulate heavy rain on dry (dry run) and wet (wet run) soil. This rainfall sequence roughly equals a rainfall event with a recurrence interval of 50 to 100 years at both test sites (Junghänel et al., 2010). During each RS run, the surface runoff was collected via the covered plot outlets (Fig. 1). From the moment that the first runoff reached the plot outlet, a water sample of 2-liters was taken every 2 min in a glass bottle with plastic-free screw caps.

Before each RS, the ploughing and rolling procedure as described in Section 2.1 was repeated to establish the same starting conditions on each plot. After soil preparation, the topsoil was sampled for bulk density and MP concentration. The bulk density was determined with the core method using standard sharpened steel  $100 \text{ cm}^3$  sized Kopecky rings (diameter 57 mm, height 40.5 mm). Before each RS, the MP

concentration of each plot was measured three times ( $\approx 50 \text{ g}$ ) from a composite topsoil ( $< 1 \text{ cm}$ ) sample taken at 10 randomly distributed plot locations to calculate the enrichment ratio (ER) comparing MP concentration of the topsoil and the sediment delivered during each RS.

$$\text{ER} = \frac{\text{mean MP concentration in sediments}}{\text{mean MP concentration in topsoil}}$$

ER values  $> 1$  indicate an enrichment, and values  $< 1$  a depletion of MP in the delivered sediment. In addition, soil moisture of the topsoil ( $< 6 \text{ cm}$ ) was measured before and 15 min after each run (dry and wet) at ten locations within each plot using a Soil Moisture Sensor (ML3 ThetaProbe, Delta-T devices, UK).

Between RSs the plots were covered with a weed tile fleece (GTM 13013,  $80 \text{ g m}^{-2}$ , color: brown, material: Polypropylene) to suppress plant growth. The water permeable fleece was stretched over the plots without surface contact. Hence, the soil was exposed to natural rain amounts but drop energy was minimized to avoid splash erosion, soil crusting and hence minimize potential surface runoff. Moreover, MP loss via wind erosion or photo degradation was avoided.

## 2.3. MP degradation and vertical fluxes

In December 2019, following the last rainfall simulation RS3, the stainless-steel cylinders were excavated (after being buried for 475 days). The soil monoliths were extracted from the cylinders and sliced into 1 cm increments. To avoid overestimation of vertical MP movement potentially resulting from preferential transport along the soil-steel interface, only an inner square section ( $12 \text{ cm} \times 12 \text{ cm}$ ) of the cylinders were analysed. It is assumed that the relative vertical loss from the soil layer of MP application (depths: 3–5 cm) in the stainless-steel cylinders represents the potential loss from the plough horizon of the plots (depths: 0–10 cm). This is acceptable as the soil was ploughed several times in the course of the experiments so that the 0–10 cm top layer can be considered to be well-mixed.

The mesh bags were also excavated (after being buried for 475 days) and quantified based on mass and the outer appearance of the  $\text{MP}_c$  particles (Section 2.5).

## 2.4. Prevention of MP contamination

To avoid MP contamination of the samples, potential contact with plastic materials was reduced to a minimum during the entire experimental process. Nevertheless, there were potential sources of MP contamination by pre-contamination of the soil, during the RS and the lab work, as there were no cleanroom conditions. To ensure that there was no pre-contamination of the plots, a 50 g composite sample out of 10 topsoil samples for each plot were taken before adding MP to the plots. Based on the procedures to extract and determine HDPE microplastic (see Sections 2.5 and 2.6), no pre-contamination with similar MP as the reference material could be found. The sediment and runoff samples were transported, dried ( $60 \text{ }^\circ\text{C}$ ) and stored in 2-liter glass jars. The only plastics used during lab work were wash bottles (PE) and the density separation unit made of polyvinyl chloride (PVC). For both wash bottles and density separator, we used colored plastic because the added MP particles were white and their color was one of the criteria used for their detection in the soil and sediment. In addition, the particle sizes of the MP particles used in this study are too large to become airborne in the laboratory. As a result, the chance of airborne contamination with similar particles during laboratory work was minimized. As we did not find any  $\text{MP}_f$  and  $\text{MP}_c$  particles in the topsoil before contaminating, generally proofs that any contamination with similar particles during sample handling is minimal to neglectable. Together with the high MP concentrations used, our method should be sufficient in avoiding remarkable sample contamination.

## 2.5. MP extraction from soil, sediment samples and mesh bags

To investigate whether the MP transport is influenced by soil aggregation, the sediment samples were separated into micro- (53–100  $\mu\text{m}$ ) and macro-aggregates (250–300  $\mu\text{m}$ ) (Fig. 2). The applied fractionation scheme follows Six et al. (1999), whereas aggregates in dried soil were separated by wet sieving through a series of two sieves (250 and 53  $\mu\text{m}$ ). The sediment samples were submerged in distilled water on top of the 250  $\mu\text{m}$  sieve for 15 min. Samples were sieved under distilled water by gently moving the sieve 3 cm vertically 50 times over a period of 2 min through distilled water in a shallow pan. The material remaining on the sieve was added to a first density separation (DS I). Sediment passing the 250  $\mu\text{m}$  sieve and remaining in the shallow pan was transferred to the 53  $\mu\text{m}$  sieve and the process was repeated. Sediment remaining on the 53  $\mu\text{m}$  sieve was also added to DS I (Fig. 2). During DS I the MP particles which were not bound to soil particles or aggregates were separated ( $\text{MP}_{\text{free}}$ ). MP together with organic material float to the surface, while the mineral soil particles and bounded MP ( $\text{MP}_{\text{bound}}$ ) particles sink to the bottom.

The density separation was performed using a Sediment-Microplastic-Isolation (SMI) unit (for details see Coppock et al., 2017). The SMI consists of 30 cm long PVC pipe with a diameter of 5 cm (volume = 0.5 l), which was hot-air bound on a PVC plate. In the centre of the pipe, a ball valve was installed to separate floating and sinking particles. The SMI was filled with distilled water (density at 20 °C:

0.998 g  $\text{cm}^{-3}$ ) as floating media and the respective soil/sediment fraction. After 12 h, the ball valve was closed and the water with the floating organic and  $\text{MP}_{\text{free}}$  particles were poured over a 350  $\mu\text{m}$  and subsequently a 53  $\mu\text{m}$  stainless steel sieve. To prevent  $\text{MP}_{\text{free}}$  particles attaching to the SMI, its upper part was extensively washed out with distilled water. Sieving through the 350  $\mu\text{m}$  sieve was performed to remove larger organic matter particles, while all  $\text{MP}_{\text{free}}$  particles ( $\text{MP}_{\text{c}}$  and  $\text{MP}_{\text{f}}$ ) should pass the sieve. Due to the second sieving through 53  $\mu\text{m}$  all  $\text{MP}_{\text{free}}$  particles remain in the sieve. From the 53  $\mu\text{m}$  sieve the  $\text{MP}_{\text{free}}$  and left organic material was poured on black colored paper filters with a diameter of 8 cm (Fig. 3 a, c). The filter size was adapted to the maximum scanning area (10 × 10 cm) of the digital microscope (Keyence VHX 6000, Japan). Black filters were used to improve the color contrast between filter and white reference MP particles. The MP and organic particles were fixed with hairspray on the still wet filter. The filters were dried at 30 °C and stored in a flat aluminium can until they were analysed with the digital microscope.

To destroy the macro- and micro-aggregates and separate  $\text{MP}_{\text{bound}}$  from soil aggregates a plastic-free magnetic stirrer was added to the under chamber of the SMI and the complete SMI was placed alternately on a magnetic stirrer plate and in an ultrasonic bath (130/300 W, 40 kHz). The dispersing procedure was as followed: 5 min magnetic stirrer, 5 min ultrasonic bath, 5 min magnetic stirrer, 5 min ultrasonic bath, short stirring pulses to stir up the settled sediment again to release trapped MP particles. After the dispersing procedure, the upper chamber of the SMI was refilled with distilled water for the second density separation DS II (Fig. 2). This releases the  $\text{MP}_{\text{bound}}$  particles that were previously bound to soil particles or incorporated in micro- and macro-aggregates (Fig. 2). As after DS I, the suspended  $\text{MP}_{\text{bound}}$  and organic material after DS II was filtered and transferred on black filters, fixed with hairspray and dried at 30 °C. The soil minerals that remained in the lower part of the SMI were dried at 105 °C. and weighed. After each density separation, the SMI was disassembled and the individual parts were first cleaned in a laboratory dishwasher and then rinsed with distilled water.

In contrast to the sediment samples, no aggregate fractionation was applied to the soil samples taken from the plots and the vertical MP movement in the steel cylinders. The dried soil samples (50 g) were wet sieved through a 2 mm sieve to remove the stone content. The sieved soil samples were mixed in 500 ml beakers filled with about 400 ml distilled water. MP potentially attached to soil aggregates, mineral substances were treated in a magnetic stirrer, and ultrasonic bath same as the sediment samples as described above. After this procedure a single density separation (DS I) was performed followed by sieving with a 350  $\mu\text{m}$  and a 53  $\mu\text{m}$  sieve and lastly placing on black colored paper filters.

The mesh bags were cleaned from soil and roots and washed with distilled water. Afterwards they were treated three times for 15 min with an ultrasonic bath (130/300 W, 400 kHz) to remove small soil particles from the  $\text{MP}_{\text{c}}$ . Afterwards the  $\text{MP}_{\text{c}}$  samples were weighted for potential weight loss and reviewed optically under the digital microscope. Therefore, we used a precision balance (Excellence Plus XP6, Mettler Toledo, USA; 0.000 mg) and a digital microscope (Keyence VHX-6000, Japan) with a magnification of 200 $\times$ .

## 2.6. Microscopic MP detection

The black paper filters with  $\text{MP}_{\text{free}}$  and  $\text{MP}_{\text{bound}}$  were analysed using a digital microscope (Keyence VHX 6000, Japan) with a magnification of 20 $\times$ , an incident light ring illumination of the 10 cm × 10 cm scan area and the ability to control the lens height (Z stage control) to adjust the focus automatically. Therefore, sharp images can be produced even when filters were uneven (Fig. 3). With a panorama scan function a whole filter can be captured in one picture (Fig. a, b). The picture was further analysed with an automatic image processing within the microscope to detect and count particles. Because the color of the particles used was known the extraction of the MP particles could be specified

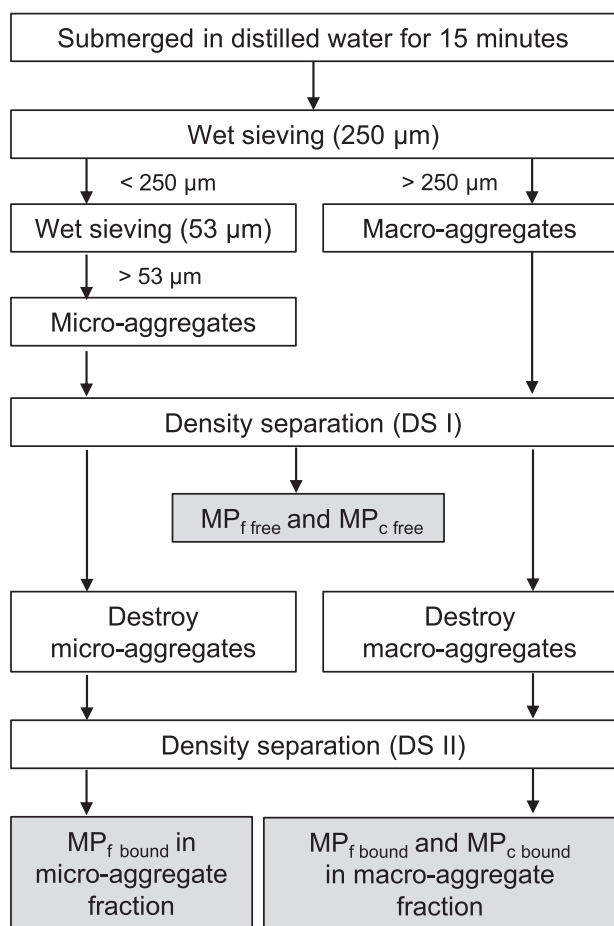


**Fig. 2.** Scheme of the laboratory extraction of high density polyethylene (HDPE) microplastic (MP) from the soil samples, considering the micro- and macro-aggregates ( $\text{MP}_{\text{free}}$  is MP not bound to soil particles and aggregates;  $\text{MP}_{\text{bound}}$  is MP bound to soil particles or aggregates).  $\text{MP}_{\text{f}}$  is fine MP, 53–100  $\mu\text{m}$ ;  $\text{MP}_{\text{c}}$  is coarse MP, 250–300  $\mu\text{m}$ . Grey boxes represent filters that have been analysed with the digital microscope.

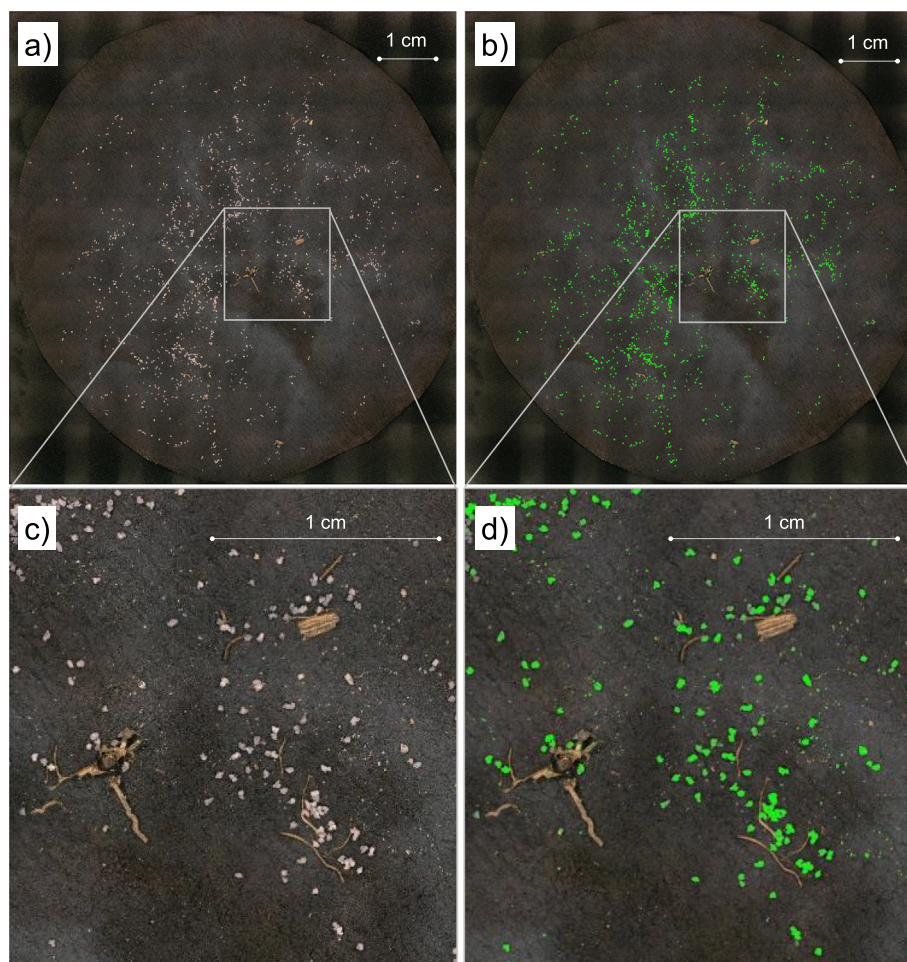


**Fig. 3.** After density separation, high density polyethylene (HDPE) microplastic (MP) and organic matter particles from the sediment samples were filtered out on black filters (a, c). For the detection of the white MP reference particles a digital microscope was used based on color. The white MP particles were captured (green = detected particles), while the brown colored organic material remained undetected (b, d).

manually according to particular image brightness, hue and saturation. The white colored HDPE microplastic was detected in its full size using brightness, saturation and hue values of 150–250, 5–50 and 0 respectively. At these settings, the organic matter could be excluded due to contrast differences (Fig. 3 b, d). A contamination of the filters through natural MP pollution of the soil was excluded by a preliminary soil sampling and high start concentration to make the possible error negligibly small (see Section 2.4).

The microscope outputs a complete size distribution ( $\mu\text{m}^2$ ) of all single detected MP particles. Further data analysis was performed in R: Development Core Team (2021). The area size distribution ( $\mu\text{m}^2$ ) of the used reference MP were known by a pronounced size distribution of the pure  $\text{MP}_f$  and  $\text{MP}_c$  via the digital microscope and amount to 1000 to 10,000  $\mu\text{m}^2$  for  $\text{MP}_f$  and 50,000 to 100,000  $\mu\text{m}^2$  for  $\text{MP}_c$  particles. Therefore, all detected particles  $<1000 \mu\text{m}^2$  were excluded. Particles  $>10,000 \mu\text{m}^2$  but  $<50,000 \mu\text{m}^2$  were interpreted as clustered  $\text{MP}_f$ . Particles  $>100,000 \mu\text{m}^2$  were interpreted as clustered  $\text{MP}_c$ . To estimate the number of single particles within a cluster, the cluster surface area was divided by the median surface area of  $\text{MP}_f$  or  $\text{MP}_c$ .

### 2.7. Quality control of MP extraction and microscopy detection

To assess the quality of the MP extraction and detection procedure, a pilot study was performed to detect the recovery rates of the reference MP particles. For this reason, soil samples of both field sites were sieved  $<2 \text{ mm}$  to remove stones and thus imitate eroded sediment samples. Afterwards 20 g soil blanks were taken and mixed with four different MP

concentrations I-IV (Table 1). For each concentration, MP size and soil type 3 replicates were prepared. The concentrations between 0.01 and 0.2  $\text{mg MP}_f \text{ g}^{-1}$  soil and 0.25–5  $\text{mg MP}_c \text{ g}^{-1}$  soil were used to cover the range of the start concentration in the field with 0.08  $\text{mg MP}_f$  and 0.38  $\text{mg MP}_c \text{ g}^{-1}$  soil. The mean recovery rate for  $\text{MP}_c$  reached  $85 \pm 1.68\%$  ( $\pm$  standard deviation,  $n = 24$ ) and  $83 \pm 5.43\%$  ( $n = 24$ ) for  $\text{MP}_f$ .

### 2.8. Statistical evaluation

The data preparation of the digital microscope, the evaluation of the MP size distribution and the test for normal distribution were carried out in R (R: Development Core Team, 2021). The statistical evaluation of the RS runs was carried out with CoStat (CoHort Software, California). All data were normally distributed (after Pearson  $K^2$  test of normality) and therefore mean values were presented per run (dry and wet run separated). To investigate if there were significant differences due to

**Table 1**

Used high density polyethylene (HDPE) microplastic (MP) concentrations (I-IV) ( $\text{mg g}^{-1}$  soil) for quality control of the microplastic extraction method. Each concentration was mixed with 20 g soil and presents 3 replicates in two soil types (total  $n = 48$ ).  $\text{MP}_f$  = fine MP, 53–100  $\mu\text{m}$ ;  $\text{MP}_c$  = coarse MP, 250–300  $\mu\text{m}$ .

	Concentration of MP ( $\text{mg g}^{-1}$ soil)			
	I	II	III	IV
$\text{MP}_f$	0.01	0.02	0.08	0.20
$\text{MP}_c$	0.25	0.50	2.50	5.00

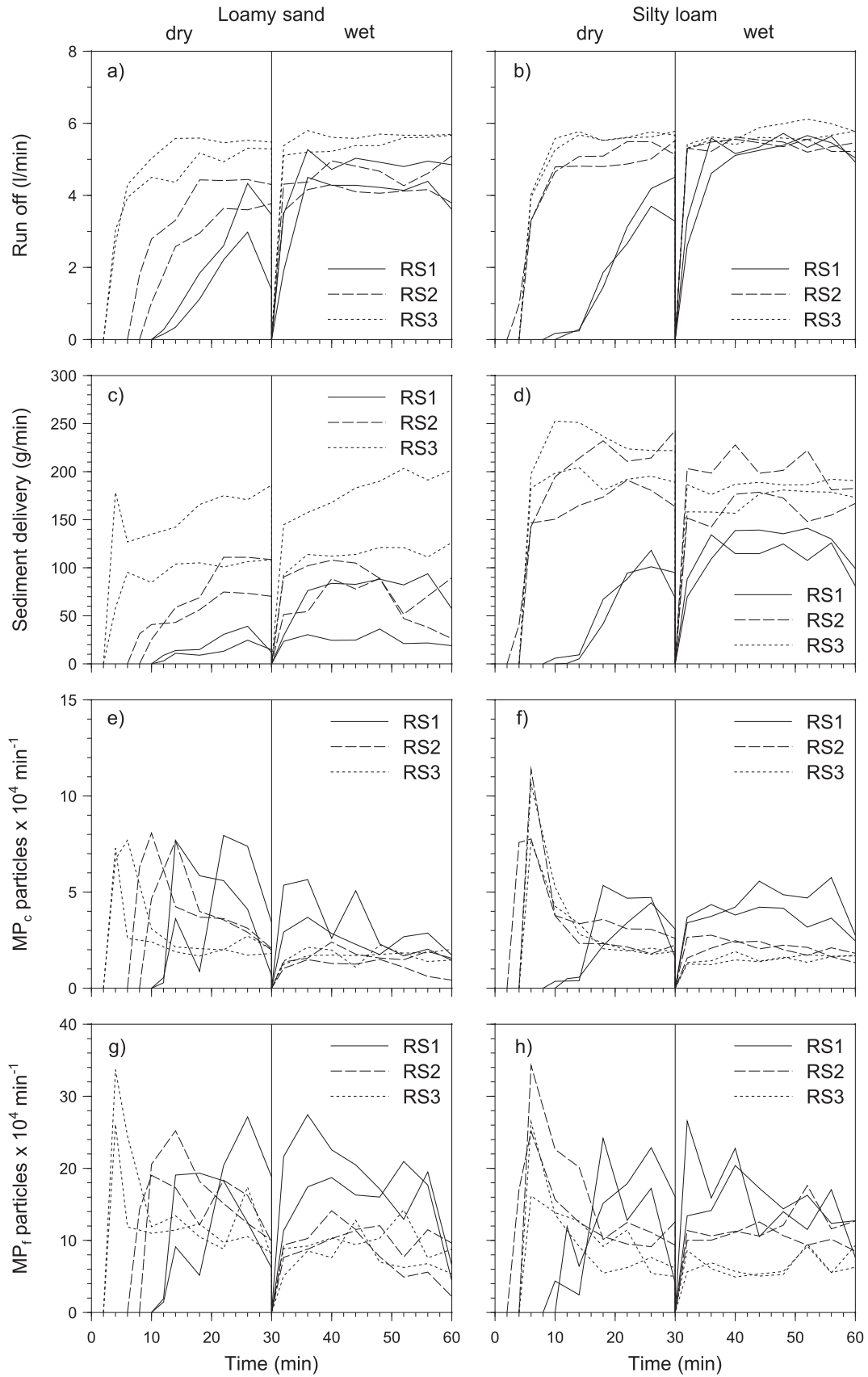


**Fig. 4.** Surface run off (a, b), sediment delivery (c, d), coarse microplastic ( $MP_c$ , 250–300  $\mu\text{m}$ ) delivery (e, f) and fine microplastic ( $MP_f$ , 53–100  $\mu\text{m}$ ) delivery (g, h) of the rainfall simulations 1, 2 and 3 (RS1, RS2 and RS3) in both soil types (silty loam and loamy sand). Each simulation is shown with two lines, which represent the two installed plots A and B on each soil type. The X-axis shows the time of a rainfall simulation run (0–30 min dry run, 30–60 min wet run).

soil type or MP size, a Welch's *t*-test (unequal variances *t*-test) was carried out to test the hypotheses of equal means ( $p < 0.05$ ). To assess the correlation between soil moisture and the sediment delivery during dry runs the Pearson correlation coefficient was used and significance evaluated at the  $p < 0.05$  level. If means are given, the variability of data is given as  $\pm$  standard deviation.

### 3. Results

#### 3.1. Surface runoff and sediment delivery

The simulations of heavy rainfall produced runoff coefficients of  $0.43 \pm 0.19$  ( $n = 12$ ) and  $0.60 \pm 0.09$  ( $n = 12$ ) for dry and wet runs, respectively. Overall, runoff rates were much more variable for the dry runs (Fig. 4 a, b) due to the high variability in soil moisture at the beginning of the RSs (Table 2). The wet runs resulted in very similar runoff rates on all plots (Fig. 4 a, b), which also corresponds to the very similar starting soil moisture conditions at the beginning of the wet runs (Table 2). Overall, mean runoff volumes during the wet runs did not significantly differ between the loamy sand and silty loam plots. It is also important to note for the interpretation of the data that the two-paired plots (A, B) of each site and simulation produce very similar runoff volumes (Fig. 4 a, b).

Sediment delivery rates of dry and wet runs in general follow the dynamics of surface runoff (Fig. 4 c, d). However, there are noteworthy differences especially in case of RS3 on loamy sand and RS2 and RS3 on silty loam were the highest sediment delivery rates were reached during the dry runs with peaks in sediment concentration up to  $253 \text{ g min}^{-1}$  at the beginning of surface runoff. In contrast to surface runoff, mean sediment delivery during wet runs differ significantly ( $p = 0.03$ ) between the soils, whereas silty loam plots were producing on average 31% more sediments. The mean sediment delivery rates during wet runs also substantially increase from RS1 to RS3 (Fig. 4 c, d). In the cases of the silty loam and the loamy sand, the sediment delivery between the first and the last wet run increased by a factor of 1.54 and 2.96, respectively. This increase was even more pronounced including the dry runs resulting in an increase by a factor of 2.27 (silty loam) and 4.45 (loamy sand), respectively. Sediment delivery during dry runs significantly correlated with soil moisture at the beginning of these simulations ( $R^2 = 0.36$ ;  $p = 0.04$ ;  $n = 82$ ).

#### 3.2. Microplastic delivery

During the dry runs, the MP concentrations were much more variable as compared to the sediment concentrations (Fig. 4). MP concentrations peaked in the first runoff reaching the plot outlets, while runoff was minimal at this stage of the experiment. Total mean delivery rates during dry and wet runs ranged between  $3 \pm 1 \cdot 10^4$  ( $n = 12$ ) and  $2.9 \pm 1.1 \cdot 10^4$   $\text{MP}_c$  particles  $\text{min}^{-1}$  ( $n = 12$ ) and  $12 \pm 3.31 \cdot 10^4$  ( $n = 12$ ) and  $13 \pm 3.47 \cdot 10^4$   $\text{MP}_f$  particles  $\text{min}^{-1}$  ( $n = 12$ ) for the silty loam and loamy sand plots, respectively (Fig. 4 e-h). During the wet runs there was no significant difference in MP delivery rates for  $\text{MP}_c$  and  $\text{MP}_f$  caused by soil type, while the total sediment delivery of the

**Table 2**

Mean soil moisture conditions measured in volume percent (vol.-%) at ten plot locations (topsoil <6 cm) before starting the rainfall simulations (RS), 15 min after the dry runs and 15 min after the wet runs; within plot moisture, variability is indicated as  $\pm$  standard deviation.

Soil	RS	Before RS (vol.-%)	After dry run (vol.-%)	After wet run (vol.-%)
Loamy sand	1	$9.86 \pm 2.35$	$35.4 \pm 3.18$	$35.4 \pm 3.56$
	2	$18.4 \pm 3.69$	$35.8 \pm 1.65$	$36.1 \pm 1.14$
	3	$34.9 \pm 2.94$	$36.6 \pm 2.19$	$41.0 \pm 2.74$
Silty loam	1	$21.1 \pm 4.22$	$35.6 \pm 3.17$	$36.1 \pm 2.92$
	2	$23.0 \pm 6.77$	$39.7 \pm 3.40$	$40.4 \pm 2.84$
	3	$33.9 \pm 3.83$	$35.4 \pm 3.52$	$37.8 \pm 2.50$

silty loam plots was significantly ( $p = 0.03$ ) larger by a factor of 1.91 as compared to the loamy sand plots. In contrast to the increasing sediment delivery between wet runs of RS1 and RS3,  $\text{MP}_c$  and  $\text{MP}_f$  delivery decreased over time at both test sites. Overall  $\text{MP}_c$  was delivered more effectively compared to  $\text{MP}_f$  (Table 3).

#### 3.3. Preferential erosion and transport of MP

The rainfall simulations showed a preferential erosion and transport of the  $\text{MP}_c$  and  $\text{MP}_f$  with a mean ER of  $3.95 \pm 3.71$  and  $3.17 \pm 2.58$  for all RSs ( $n = 24$ ), respectively (Fig. 5). Despite the larger mean in case of  $\text{MP}_c$ , the size of MP did not show any significant difference due to the high variability between all the runs (Fig. 5). Even more pronounced differences were found between the two soil types with substantially larger mean MP ER in case of loamy sand ( $\text{MP}_c$  ER =  $5.90 \pm 4.38$ ;  $\text{MP}_f$  ER =  $4.72 \pm 2.76$ ;  $n = 12$ ) compared to the mean MP ER of silty loam ( $\text{MP}_c$  ER =  $1.99 \pm 0.77$ ;  $\text{MP}_f$  ER =  $1.63 \pm 0.99$ ;  $n = 12$ ). These differences were also not significant due to the high variability of the single sample values (Fig. 5). Overall, the enrichment factors for  $\text{MP}_c$  and  $\text{MP}_f$  were substantially higher and more variable during dry runs ( $\text{MP}_c$  ER =  $5.45 \pm 4.48$ ;  $\text{MP}_f$  ER =  $3.90 \pm 2.93$ ;  $n = 12$ ) compared to the wet runs ( $\text{MP}_c$  ER =  $2.43 \pm 1.69$ ;  $\text{MP}_f$  ER =  $2.44 \pm 1.94$ ;  $n = 12$ ) ( $p < 0.01$ ).

The sediment fractionation and two-step density separation (Fig. 2) clearly show an increasing interaction between MP and mineral particles over time (Fig. 6). However, this interaction was more dominant in the case of  $\text{MP}_f$  bound ( $53.9 \pm 12.5\%$  of particles were bound to soil minerals;  $n = 24$ ) compared to  $\text{MP}_c$  bound ( $26.4 \pm 12.9\%$  of particles were bound to soil minerals;  $n = 24$ ) ( $p < 0.01$ ). Considered across all RSs, no significant difference could be found between the two soil types with regard to the interaction between  $\text{MP}_c$  or  $\text{MP}_f$  and soil. However, including the chronological sequence from RS1 to RS3, there was a significantly higher interaction between  $\text{MP}_f$  and soil minerals/aggregates in the silty loam during RS1 ( $p = 0.03$ ) but not in RS2 and RS3. For  $\text{MP}_c$ , also the MP-soil interaction was more pronounced for the finer soil matrix (silty loam) but only was significant in RS3 ( $p = 0.03$ ). Over time, significant differences disappear in case of  $\text{MP}_f$  and arise in case of  $\text{MP}_c$ . No significant difference in the interaction between  $\text{MP}_c/\text{MP}_f$  and soil minerals and/or aggregates was found between the dry and wet runs. During the last simulation (RS3)  $38.9 \pm 10.2\%$  ( $\text{MP}_c$  bound;  $n = 8$ ) and  $62.1 \pm 13.1\%$  ( $\text{MP}_f$  bound;  $n = 8$ ) of the eroded MP was bound to soil particles or aggregates.

#### 3.4. Degradability and vertical movement

As expected, no significant degradation of the used HDPE particles was found after being buried in soil for 475 days. The weight of the  $\text{MP}_c$  buried slightly increased (mean difference +  $2.03 \pm 1.03\%$ ;  $n = 6$ ) because attached clay particles could not be fully removed with the ultrasonic treatment. There was also no visible change in particle surface using a microscopy magnification of  $200\times$ .

**Table 3**

Mean lateral microplastic ( $\text{MP}_f$  = fine MP, 53–100  $\mu\text{m}$ ;  $\text{MP}_c$  = coarse MP, 250–300  $\mu\text{m}$ ) loss after rainfall simulation 1, 2 and 3 (RS1, RS2 and RS3) and mean vertical  $\text{MP}_c$  and  $\text{MP}_f$  loss (steel cylinders) relative to  $\text{MP}_c$  and  $\text{MP}_f$  amounts added to topsoil at the beginning of the experiment in percent. The lateral loss presents the mean of two plots per soil type ( $n = 2$ ), vertical loss presents mean  $\pm$  standard deviation of three pipes per soil type ( $n = 3$ ).

	Rainfall simulation plots				Steel cylinders
	Lateral loss (%)				Vertical loss (%)
	RS1	RS2	RS3	Total	
$\text{MP}_c$					
Silty loam	4.70	4.65	4.01	12.8	$1.51 \pm 1.67$
Loamy sand	4.80	3.86	3.75	11.9	$2.95 \pm 1.17$
$\text{MP}_f$					
Silty loam	0.79	0.80	0.50	2.08	$5.01 \pm 1.67$
Loamy sand	0.84	0.68	0.67	2.18	$5.87 \pm 3.20$

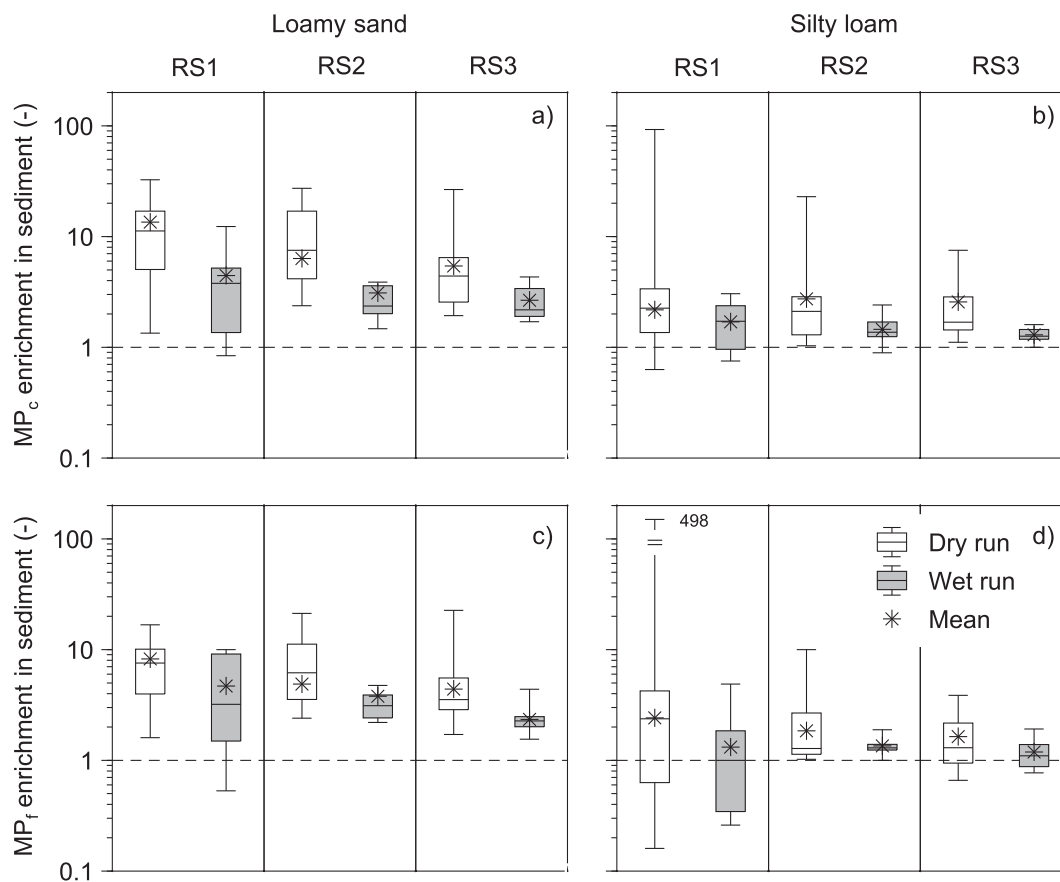


**Fig. 5.** Microplastic (MP) enrichment ratios of coarse MP ( $MP_c$ , 250–300  $\mu\text{m}$ ) particles (a, b) and fine MP ( $MP_f$ , 53–100  $\mu\text{m}$ ) particles (c, d) in the delivered sediment of two soil types (loamy sand and silty loam) during the rainfall simulations 1, 2 and 3 (RS1, RS2 and RS3). A preferential erosion of MP is shown by a mean enrichment factor >1 in all simulations. Boxes present all single sample values during the runs and show the median and the 1st and 3rd quartile, whiskers give the minimum and maximum; the stars present mean values per run; the dashed line indicates the relative initial concentration in topsoil < 1 cm (factor 1).

The observation of the vertical MP movement in the stainless steel cylinders showed an average  $MP_c$  loss of  $1.51 \pm 1.67\%$  ( $n = 3$ ) and  $2.95 \pm 1.17\%$  ( $n = 3$ ) to soil depths below the MP application layer (3–5 cm) for silty loam and loamy sand, respectively. This vertical transfer was more pronounced for  $MP_f$ , whereas  $5.01 \pm 1.67\%$  ( $n = 3$ ) for silty loam and  $5.87 \pm 3.20\%$  ( $n = 3$ ) for loamy sand of applied MP was found below a soil depth of 5 cm.

## 4. Discussion

### 4.1. Preferential erosion and transport of MP

In case of the MP particles tested in our experiment (diameter 53–100  $\mu\text{m}$  and 250–300  $\mu\text{m}$ , density  $0.957 \text{ g cm}^{-3}$ ) we found preferential erosion and transport in comparison to the mineral soil, reflected in a mean enrichment ratio > 1 during all RSs (Fig. 5). This verifies our hypothesis that less dense materials are preferentially eroded and transported. We are not aware of any comparable results on water erosion of MP, but our results are in line with experimental findings focusing on particulate organic matter (POM) erosion (also with densities below  $1.0 \text{ g cm}^{-3}$ ). For example, Martínez-Mena et al. (2012), Müller-Nedebeck and Chaplot (2015) and Wang et al. (2013) found POM enrichment ratios between 1.37 and 2.9. Recent work on the mobilization of MP by wind erosion also confirmed the preferential MP transport of 212  $\mu\text{m}$  particles with enrichment factors of up to 5 due to the low density (Bullard et al., 2021).

A higher enrichment of  $MP_c$  in the delivered sediment can be explained by the less pronounced connection to soil particles. Based on the analysis of  $MP_{\text{free}}$  and  $MP_{\text{bound}}$  (Fig. 6) it is obvious that there are

stronger binding forces between the smaller  $MP_f$  compared to the coarser  $MP_c$  and the mineral soil, a fact which generally can be found for smaller soil particles (He et al., 2008; Hu et al., 2015; Wagner et al., 2007). This association of MP with soil minerals leads to a less pronounced density-induced MP enrichment in delivered sediments, with a greater effect on  $MP_f$ . This is also mirrored in the less pronounced MP enrichment ratios in case of the silty loam (Fig. 5 b, d) even in case of the first runs where encapsulation in aggregates can be neglected.

A smaller enrichment of  $MP_f$  in general in delivered sediments, might be also an indication of aggregation and encapsulating in aggregates, e.g. following repeated dry and wetting cycles, which might play an important role for the more limited erosion and transport of fine MP particles. By splitting the topsoil (before the RS sequence started) into the different size fractions used for sediment analysis (Section 2.5), we can assume a potential depletion of micro- (water stable) and macro-aggregates (non-water stable) in delivered sediments ( $ER < 1$ ). Whereas, comparing the sediment size fraction <53  $\mu\text{m}$  with the soil fraction <53  $\mu\text{m}$  give some indication that, as expected, non-aggregated particles are preferentially eroded (ER of sediments <53  $\mu\text{m}$  vs. soil fraction <53  $\mu\text{m}$ ;  $1.73 \pm 0.44$  and  $2.10 \pm 1.01$  in case of silty loam and loamy sand, respectively). Overall, our data indicate that the  $MP_f$  used in this study is more strongly bound to mineral particles and may also be encapsulated in water stable aggregates. The latter effect cannot be found in case of the  $MP_c$ , which might be encapsulated in larger aggregates (> 250  $\mu\text{m}$ ), as the larger soil aggregates are less water stable (Angers et al., 2008; Lal, 2015; Six et al., 1999) and hence are potentially destroyed during erosion and transport.

Overall, MP erosion should be substantially affected by aggregation between MP and mineral soil particles of different size and properties.

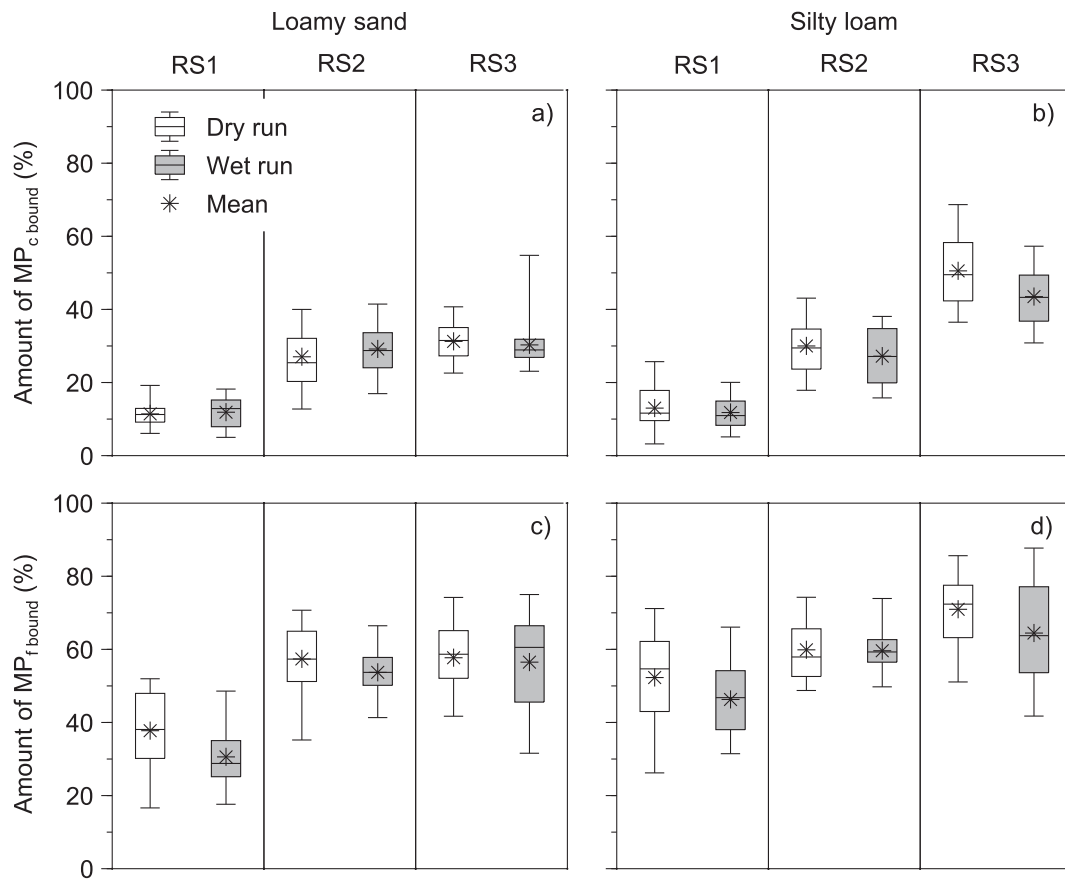


**Fig. 6.** The increasing amount of coarse microplastic ( $MP_{c, bound}$ , 250–300  $\mu m$ ) particles (a, b) and fine microplastic ( $MP_{f, bound}$ , 53–100  $\mu m$ ) particles (c, d) in the delivered sediment which was bound to soil particles or aggregates during the rainfall simulations 1, 2 and 3 (RS1, RS2 and RS3) on two soil types (loamy sand and silty loam). Boxplots present all single sample values during the rainfall simulation runs and show the median and the 1st and 3rd quartile, whiskers give the minimum and maximum; the stars present mean values per run.

The general tendency to build aggregates was already shown in earlier laboratory studies indicating both a high intra (with one another) and inter (with organic matter) binding potential of MP in soils (Bastos and De las Nieves, 1994; Bouchard et al., 2013; Walker and Bob, 2001). Zhang and Liu (2018) observed up to 72% of MP particles (> 500  $\mu m$ ) associated with soil aggregates in Nitisol and Gleysol in a semi-humid region of China. Even if such large aggregates might not be stable during erosion processes, their findings confirm the general importance of aggregation in MP stabilisation in the soil.

It is also important to note that the ER of MP during erosion and transport was generally more pronounced for the dry runs as compared to the following wet runs. This might have two reasons: (i) Loose,  $MP_{free}$  on the soil surface resulting from the tillage of the plots before each RS sequence might be flashed out during the dry runs. This assumption is partly underlined through the highest MP concentrations measured right at the beginning of the dry runs (Fig. 4 f, h). (ii) There might be some additional binding forces between wet MP and wet mineral particles in case of the pre-wetted soils in case of the wet runs. This would be consistent with findings of several studies indicating stronger binding forces between soil particles under wet conditions (Lehrsch and Jolley, 1992; Luk, 1983; Swanson and Dedrick, 1967).

#### 4.2. Change in MP delivery over time

Over the 1.5 years of the experiment, the enrichment ratio in the consecutive rainfall simulations decreased for both particle sizes (Fig. 5). This decrease in ER is mirrored in an increase in the amount of  $MP_{f, bound}$  and  $MP_{c, bound}$  in the delivered sediments over time (Fig. 6).

The near constant mass flux of MP over time for all experiments resulted from decreasing MP concentrations in delivered sediments

whereas overall erosion and sediment delivery increased (Fig. 4). This increase in sediment delivery over time, most likely results by chance from an increasing soil moisture between RS1 to RS3 (Table 2). Interestingly, even under similar initial topsoil moisture conditions (Table 2) and similar surface runoff in case of the wet runs (Fig. 4 a, b), we still found an increase in sediment delivery with a factor of 1.54 (silty loam) and 2.96 (loamy sand) between RS1 and RS3. This might result from an increase of sediment connectivity (Boardman et al., 2019) during these wet runs due to the more substantial erosion during the dry runs in case of higher initial soil moisture conditions (Fig. 4 c, d; Table 2).

While the MP concentrations in delivered sediments decreased over time, the total delivery of MP per (wet) run was more or less stable for all runs and both soils. The near equal  $MP_c$  and  $MP_f$  delivery in case of both soils occurred by chance from the combination of lower MP enrichment in case of silty loam (Fig. 5 b, d) and the higher erodibility of silty soils leading to more erosion and sediment delivery (Fig. 4 c, d). However, it is important to note that our results indicate that even sandy soils, typically not classified as very erodible, might be a substantial MP source.

The MP concentrations in delivered sediments declined over time due to decreasing enrichment caused by MP-soil binding and/or aggregation and a general reduction of topsoil MP concentrations. The latter has two main reasons: (i) Topsoil MP concentrations declined due to lateral loss with surface runoff and erosion. Compared to the start conditions, there was a total loss (dry and wet runs) of  $5.20 \cdot 10^6$   $MP_c$  particles (12.8%) per plot on silty loam ( $n = 2$ ) and  $4.86 \cdot 10^6$   $MP_c$  particles (11.9%) on loamy sand ( $n = 2$ ) over all RSs (Table 3). This results in an average  $MP_c$  loss of 4.25% (on silty loam) and 3.98% (on loamy sand) per heavy rain event. For  $MP_f$  there was a total loss of  $21.2 \cdot 10^6$

particles (2.08%) per plot on silty loam ( $n = 2$ ) and  $22.2 \cdot 10^6$  particles (2.18%) on loamy sand ( $n = 2$ ) (Table 3). This leads to a mean  $MP_f$  loss of 0.69% (on silty loam) and 0.73% (on loamy sand) for a single heavy rain event. (ii) Topsoil MP concentrations declined over time due to vertical loss below the plough layer. Vertical MP transport via infiltration and bioturbation is widely discussed and partly observed in earlier studies, e.g. Rillig et al. (2017b), whereas especially earthworms play an important role in directly transporting MP via digestion and excretion (Huerta Lwanga et al., 2016; Huerta Lwanga et al., 2018) or in preparing preferential flow pathways for MP leaching (Yu et al., 2019). In our study, the added  $MP_c$  and  $MP_f$  was found up to a depth of 0.42 m in the soil column. The overall loss within 1.5 years from the application horizon (3–5 cm) was  $1.51 \pm 1.67\%$  and  $2.95 \pm 1.17\%$  as well as  $5.01 \pm 1.67\%$  to  $5.87 \pm 3.20\%$  ( $n = 3$ ) for the  $MP_c$  and  $MP_f$  in the silty loam and loamy sand, respectively. This clearly indicates that in case of soils prone to erosion larger  $MP_c$  particles are dominantly lost via soil erosion, while for small  $MP_f$  particles erosion is less important and moreover these particles are slowly but steadily moved below the plough horizon.

#### 4.3. Experimental and environmental behavior

Through the experiment design of this study, the investigated transport behavior of the MP particles relates mainly to processes of interrill erosion. The analysed enrichment of the MP in the delivered sediment must be seen in connection with the plot size. On a landscape scale a different extend of enrichment or depletion of MP in delivered sediments might occur due to two opposing processes: (i) Non-selective rill and ephemeral gully erosion may play an important role at the hillslope to catchment scale leading to a reduction of interrill erosion-induced MP enrichment, while (ii) preferential deposition of heavier mineral particles within the landscape should increase the enrichment of MP in sediments delivered to surface water bodies. To our knowledge there are no MP studies available to proof this, however, there is some analogy to the processes of erosion, transport and deposition of soil organic carbon, which also shows enrichment on the plot to catchment scale (Bertol et al., 2007; Rhoton et al., 2006).

In our study, we analysed HDPE particles of one material in two size fractions only, so it is the question if results of our study can be generalized. Obviously, other MP particles with similar size, shape and density should show a somewhat similar behavior during erosion processes. As the most commonly used plastics materials alongside HDPE, other PE types, polypropylene (PP) and polystyrene (PS) (Koutnik et al., 2021) all have lower densities than mineral soils. There should be a similar size dependent preferential erosion as long as these particles have a similar shape as the tested HDPE. There might be some differences in case of the heavier polyethylene terephthalate (PET) (density up to  $1.67 \text{ g cm}^{-3}$ ), especially in depositional areas where particles substantially heavier than water might settle.

Although there are many similar properties, the polymers behave differently under certain chemical conditions. For example, sorption behavior of MP depends on the pH value. While PS is negatively charged with a pH solution below 7.1 the sorption behavior of PE and PP keeps more stable and negative up to a pH of 11 (Guo et al., 2018). On the field sides of this study the pH was 7.1 (silty loam) and 6.9 (loamy sand) which could cause different kinetic sorption to the soil particles due to type of polymer. Maybe PS would be more easily eroded due to a reduced sorption behavior compared to PE (Chen et al., 2021; Guo et al., 2018).

Another important aspect is the shape of the MP. Especially, in case of fibers typically found in sewage sludge (Bayo et al., 2016; Carr et al., 2016; Zubris and Richards, 2005) a more conservative erosion and transport behavior would be expected. However, this is somewhat speculative and obviously calls for more research to shed light on erosion as pathway of MP from soils to surface water bodies.

## 5. Conclusion

This study analysed the behavior of a known MP contamination in soils during the process of soil erosion in a long-term plot experiment where a series of controlled rainfall simulations were carried out. In general, HDPE particles of a diameter between 53–100  $\mu\text{m}$  and 250–300  $\mu\text{m}$  were preferentially eroded and transported leading to a mean enrichment ratio of  $3.17 \pm 2.58$  ( $n = 12$ ) and  $3.95 \pm 3.71$  ( $n = 12$ ) in the eroded sediment, respectively.

For both MP fractions the ER decline from RS1 to RS3. This clearly indicates that MP-soil interactions (binding and/or aggregation in water stable aggregates in case of fine materials) play a crucial role in MP erosion. This is also underlined through the differences in MP concentrations in delivered sediments depending on soil texture, with lower concentrations in more fine textured soils. The combination of lower MP concentrations in delivered sediments from the finer textured silty loam, with the higher erosion rates of these soils, leads finally to similar MP fluxes from the silty loam and the loamy sand plots. Therefore, it is important to note that coarse textured soils, typically not assumed to be very erosive, still exhibit a substantial potential of MP erosion.

Taking lateral MP loss via erosion and vertical redistribution of MP below the plough layer into account clearly indicates that the MP source-sink function strongly depends on MP particle size. In our experiment,  $MP_c$  was predominantly lost via erosion-induced lateral transport while the  $MP_f$  was predominantly redistributed below the plough layer and hence protected from further soil erosion.

There is still a lack of knowledge about the behavior of the MP particles during runoff and erosion events to estimate realistic MP inputs from arable land to inland waters. The results of this study allows some first estimates of transport behavior of HDPE particles during soil erosion and show relevant interactions due the behavior of MP in agriculture soils. Especially, the binding to soil minerals, its incorporation in aggregates and the vertical transport below the plough layer were important observations to understand the fate of MP in soil. However, especially the MP/soil interactions need to be studied for a larger range of MP shapes and chemical properties. Moreover, it is important to note that the plot experiments focused on interrill erosion cannot be straight away transferred to the catchment scale as other erosion and especially deposition processes will dominate on this scale. Overall, our results indicate that soil erosion can be a substantial source of MP entering neighboring ecosystems. Simply combining existing erosion estimates or modelling approaches with potential soil MP contaminations is not sufficient, as our knowledge of MP/soil interactions leading to preferential or more conservative behavior of MP during erosion, transport and deposition processes is very limited.

#### CRediT authorship contribution statement

Raphael Rehm: Writing - Original Draft, Visualization, Methodology  
 Arthur Schmidt: Resources, Investigation  
 Tabea Zeyer: Methodology, Validation  
 Peter Fiener: Writing Review & Editing, Conceptualization, Supervision

#### Declaration of competing interest

The authors declare that they have no known competing financial interests or personal relationships that could have appeared to influence the work reported in this paper.

#### Acknowledgments

The authors would like to acknowledge the financial support from the Federal Ministry of Education and Research towards this research as part of the initiative Plastics in the Environment (funding number 02WPL1447A-G). Additionally, we acknowledge the support of the Bavarian State Research Centre for Agriculture and the Technical

University of Munich for providing access to test plots and supporting our fieldwork at their experimental farms in Strass and Freising. Lastly, special thanks go to the members of the Soil and Water Resource Research Group in Augsburg for their assistance during the rainfall simulations.

## References

- Ajith, N., Arumugam, S., Parthasarathy, S., Manupoori, S., Janakiraman, S., 2020. Global distribution of microplastics and its impact on marine environment—a review. *Environ. Sci. Pollut. Res.* 29, 25970–25986.
- Angers, D.A., Bullock, M., Mehuys, G., 2008. Aggregate stability to water. *Soil Sampling and Methods of Analysis 2*, 811–819.
- Auerswald, K., Kainz, M., Schröder, D., Martin, W., 1992. Comparison of German and Swiss rainfall simulators—experimental setup. *Z. Pflanzenernähr. Bodenkd.* 155, 1–5.
- Baensch-Baltruschat, B., Kocher, B., Kochleus, C., Stock, F., Reifferscheid, G., 2020. Tyre and road wear particles—a calculation of generation, transport and release to water and soil with special regard to German roads. *Sci. Total Environ.* 752, 141939.
- Bastos, D., De las Nieves, F., 1994. Colloidal stability of sulfonated polystyrene model colloids. Correlation with electrokinetic data. *Colloid Polym. Sci.* 272, 592–597.
- Bayo, J., Olmos, S., López-Castellanos, J., Alcolea, A., et al., 2016. Microplastics and microfibers in the sludge of a municipal wastewater treatment plant. *Int. J. Sustain. Dev. Plan.* 11, 812–821.
- Bertol, I., Engel, F., Mafra, A., Bertol, O., Ritter, S., 2007. Phosphorus, potassium and organic carbon concentrations in runoff water and sediments under different soil tillage systems during soybean growth. *Soil Tillage Res.* 94, 142–150.
- Besseling, E., Quik, J.T.K., Sun, M., Koelmans, A.A., 2017. Fate of nano- and microplastic in freshwater systems: a modeling study. *Environ. Pollut.* 220, 540–548.
- Blasing, M., Amelung, W., 2018. Plastics in soil: analytical methods and possible sources. *Sci. Total Environ.* 612, 422–435.
- Boardman, J., Vandaele, K., Evans, R., Foster, I.D., 2019. Off-site impacts of soil erosion and runoff: why connectivity is more important than erosion rates. *Soil Use Manag.* 35, 245–256.
- Bouchard, D., Zhang, W., Chang, X., 2013. A rapid screening technique for estimating nanoparticle transport in porous media. *Water Res.* 47, 4086–4094.
- Braun, M., Mail, M., Heyse, R., Amelung, W., 2020. Plastic in compost: prevalence and potential input into agricultural and horticultural soils. *Sci. Total Environ.* 760, 143335.
- Bullard, J.E., Ockelford, A., O'Brien, P., Neuman, C.M., 2021. Preferential transport of microplastics by wind. *Atmos. Environ.* 245, 118038.
- Carr, S.A., Liu, J., Tesoro, A.G., et al., 2016. Transport and fate of microplastic particles in wastewater treatment plants. *Water Res.* 91, 174–182.
- Castro-Jiménez, J., González-Fernández, D., Fornier, M., Schmidt, N., Sempé, R., et al., 2019. Macro-litter in surface waters from the Rhone River: plastic pollution and loading to the NW Mediterranean Sea. *Mar. Pollut. Bull.* 146, 60–66.
- Chen, X., Gu, X., Bao, L., Ma, S., Mu, Y., et al., 2021. Comparison of adsorption and desorption of triclosan between microplastics and soil particles. *Chemosphere* 263, 127947.
- Coppock, R.L., Cole, M., Lindeque, P.K., Queirós, A.M., Galloway, T.S., 2017. A small-scale, portable method for extracting microplastics from marine sediments. *Environ. Pollut.* 230, 829–837.
- Corradini, F., Meza, P., Eguiluz, R., Casado, F., Huerta-Lwanga, E., Geissen, V., 2019. Evidence of microplastic accumulation in agricultural soils from sewage sludge disposal. *Sci. Total Environ.* 671, 411–420.
- Crossman, J., Hurley, R.R., Futter, M., Nizzetto, L., 2020. Transfer and transport of microplastics from biosolids to agricultural soils and the wider environment. *Sci. Total Environ.* 724, 138334.
- da Costa, J.P., Paco, A., PSM, Santos, Duarte, A.C., Rocha-Santos, T., 2019. Microplastics in soils: assessment, analytics and risks. *Environ. Chem.* 16, 18–30.
- de Souza Machado, A.A., Lau, C.W., Till, J., Kloas, W., Lehmann, A., Becker, R., et al., 2018. Impacts of microplastics on the soil biophysical environment. *Environ. Sci. Technol.* 52, 9656–9665.
- Dris, R., Gasperi, J., Rocher, V., Saad, M., Renault, N., Tassin, B., 2015. Microplastic contamination in an urban area: a case study in greater Paris. *Environ. Chem.* 12, 592–599.
- Espí, E., Salmerón, A., Fontecha, A., García, Y., Real, A.I., 2016. PLastic films for agricultural applications. *J. Plast. Film Sheeting* 22, 85–102.
- Gasperi, J., Wright, S.L., Dris, R., Collard, F., Mandin, C., Guerrouache, M., et al., 2018. Microplastics in air: are we breathing it in? *Current Opinion in Environmental Science & Health* 1, 1–5.
- Guo, X., Pang, J., Chen, S., Jia, H., et al., 2018. Sorption properties of tylosin on four different microplastics. *Chemosphere* 209, 240–245.
- He, Y.T., Wan, J., Tokunaga, T., 2008. Kinetic stability of hematite nanoparticles: the effect of particle sizes. *J. Nanopart. Res.* 10, 321–332.
- Horton, A.A., Walton, A., Spurgeon, D.J., Lahive, E., Svendsen, C., 2017. Microplastics in freshwater and terrestrial environments: evaluating the current understanding to identify the knowledge gaps and future research priorities. *Sci. Total Environ.* 586, 127–141.
- Hu, F., Xu, C., Li, H., Li, S., Yu, Z., Li, Y., et al., 2015. Particles interaction forces and their effects on soil aggregates breakdown. *Soil Tillage Res.* 147, 1–9.
- Huerta Lwanga, E., Gertsen, H., Gooren, H., Peters, P., Salanki, T., van der Ploeg, M., et al., 2016. Microplastics in the terrestrial ecosystem: implications for *Lumbricus terrestris* (Oligochaeta, Lumbricidae). *Environ. Sci. Technol.* 50, 2685–2691.
- Huerta Lwanga, E., Thapa, B., Yang, X.M., Gertsen, H., Salanki, T., Geissen, V., et al., 2018. Decay of low-density polyethylene by bacteria extracted from earthworm's guts: a potential for soil restoration. *Sci. Total Environ.* 624, 753–757.
- Junghänel, T., Ertel, H., Deutschländer, T., Wetterdienst, D., 2010. KOSTRA-DWD-2010R. Bericht zur Revision der koordinierten Starkregenregionalisierung und-auswertung des Deutschen Wetterdienstes in der Version.
- Kainz, M., Eicher, A., 1991. Der Weihenstephaner Schwenkdüsenregner. Manuskript. Lehrstuhl für Bodenkunde der TU München.
- Kainz, M., Auerswald, K., Vöhringer, R., 1992. Comparison of German and Swiss rainfall simulators—utility, labour demands and costs. *Zeitschrift fuer Pflanzenernaehrung und Bodenkunde (Germany, FR)*.
- Koelmans, A.A., NHM, Nor, Hermesen, E., Kooi, M., Mintenig, S.M., De France, J., 2019. Microplastics in freshwaters and drinking water: critical review and assessment of data quality. *Water Res.* 155, 410–422.
- Koutnik, V.S., Leonard, J., Alkidim, S., DePrima, F., Ravi, S., Hoek, E., et al., 2021. Distribution of microplastics in soil and freshwater environments: global analysis and framework for transport modeling. *Environ. Pollut.* 274, 116552.
- Lal, R., 2015. Restoring soil quality to mitigate soil degradation. *Sustainability* 7, 5875–5895.
- Lambert, S., Wagner, M., 2018. Microplastics are contaminants of emerging concern in freshwater environments: an overview. *Freshwater Microplastics* 1–23.
- Lehrsch, G.A., Jolley, P.M., 1992. Temporal changes in wet aggregate stability. *Trans. Am. Soc. Agric. Eng.* 35, 493–498.
- Li, J., Song, Y., Cai, Y., 2020. Focus topics on microplastics in soil: analytical methods, occurrence, transport, and ecological risks. *Environ. Pollut.* 257, 113570.
- Li, R.L., Zhang, L.L., Xue, B.M., Wang, Y.H., 2019. Abundance and characteristics of microplastics in the mangrove sediment of the semi-enclosed Maowei Sea of the South China Sea: new implications for location, rhizosphere, and sediment compositions. *Environ. Pollut.* 244, 685–692.
- Liu, L.-Y., Mai, L., Zeng, E.Y., 2020. Plastic and Microplastic Pollution: From Ocean Smog to Planetary Boundary Threats. A New Paradigm for Environmental Chemistry and Toxicology. Springer, pp. 229–240.
- Luk, S.H., 1983. Effect of aggregate size and microtopography on rainwash and rainsplash erosion. *Z. Geomorphol.* 27, 283–295.
- Mai, L., Bao, L.-J., Wong, C.S., Zeng, E.Y., 2018. Microplastics in the terrestrial environment. *Microplastic Contamination in Aquatic Environments*. Elsevier, pp. 365–378.
- Martínez-Mena, M., López, J., Almagro, M., Albaladejo, J., Castillo, V., Ortiz, R., et al., 2012. Organic carbon enrichment in sediments: effects of rainfall characteristics under different land uses in a Mediterranean area. *Catena* 94, 36–42.
- Moeller, J.N., Löder, M.G., Laforsch, C., 2020. Finding microplastics in soils—a review of analytical methods. *Environ. Sci. Technol.* 54, 2078–2090.
- Muller-Nedebock, D., Chaplot, V., 2015. Soil carbon losses by sheet erosion: a potentially critical contribution to the global carbon cycle. *Earth Surf. Process. Landf.* 40, 1803–1813.
- Ng, E.L., Lwanga, E.H., Eldridge, S.M., Johnston, P., Hu, H.W., Geissen, V., et al., 2018. An overview of microplastic and nanoplastic pollution in agroecosystems. *Sci. Total Environ.* 627, 1377–1388.
- Nizzetto, L., Bussi, G., Futter, M.N., Butterfield, D., Whitehead, P.G., 2016a. A theoretical assessment of microplastic transport in river catchments and their retention by soils and river sediments. *Environ. Sci.: Processes Impacts* 18, 1050–1059.
- Nizzetto, L., Futter, M., Langaas, S., 2016b. Are agricultural soils dumps for microplastics of urban origin? *Environ. Sci. Technol.* 50, 10777–10779.
- Piehl, S., Leibner, A., Loder, M.G.J., Dris, R., Bogner, C., Laforsch, C., 2018. Identification and quantification of macro- and microplastics on an agricultural farmland. *Sci. Rep.* 8.
- Qi, Y.L., Beriot, N., Gort, G., Lwanga, E.H., Gooren, H., Yang, X.M., et al., 2020. Impact of plastic mulch film debris on soil physicochemical and hydrological properties. *Environ. Pollut.* 266.
- R: Development Core Team, 2021. R: A Language and Environment Interaction for Statistical Computing. R Foundation for Statistical Computing, Vienna, Austria.
- Rehm, R., Grashy-Jansen, S., Thalheimer, M., 2018. Plastik im Boden. Ein noch unbekanntes Problem im Obst- und Weinbau? *obstbau weinbau*. vol. 11 pp. 13–16.
- Rhoton, F., Emmerich, W., Goodrich, D., Miller, S., McChesney, D., 2006. Soil geomorphological characteristics of a semiarid watershed: influence on carbon distribution and transport. *Soil Sci. Soc. Am. J.* 70, 1532–1540.
- Rillig, M.C., Bonkowski, M., 2018. Microplastic and soil protists: a call for research. *Environ. Pollut.* 241, 1128–1131.
- Rillig, M.C., Lehmann, A., 2020. Microplastic in terrestrial ecosystems. *Science* 368, 1430–1431.
- Rillig, M.C., Ingrassia, R., AAD, Machado, 2017a. Microplastic incorporation into soil in agroecosystems. *Front. Plant Sci.* 8.
- Rillig, M.C., Ziersch, L., Hempel, S., 2017b. Microplastic transport in soil by earthworms. *Sci. Rep.* 7, 1362.
- Rochman, C.M., 2018. Microplastics research—from sink to source. *Science* 360, 28–29.
- Saling, P., Gyuzelova, L., Wittstock, K., Wessolowski, V., Griesshammer, R., 2020. Life cycle impact assessment of microplastics as one component of marine plastic debris. *Int. J. Life Cycle Assess.* 1–19.
- Six, J., Elliott, E., Paustian, K., 1999. Aggregate and soil organic matter dynamics under conventional and no-tillage systems. *Soil Sci. Soc. Am. J.* 63, 1350–1358.
- Stolte, A., Forster, S., Gerdt, G., Schubert, H., 2015. Microplastic concentrations in beach sediments along the German Baltic coast. *Mar. Pollut. Bull.* 99, 216–229.
- Swanson, N.P., Dedrick, A.R., 1967. Soil particles and aggregates transported in water runoff under various slope conditions using simulated rainfall. *Trans. Am. Soc. Agric. Eng.* 10, 246–247.
- Tagg, A.S., do Sul, J.A.I., 2019. Is this your glitter? An overlooked but potentially environmentally-valuable microplastic. *Mar. Pollut. Bull.* 146, 50–53.
- van den Berg, P., Huerta-Lwanga, E., Corradini, F., Geissen, V., 2020. Sewage sludge application as a vehicle for microplastics in eastern Spanish agricultural soils. *Environ. Pollut.* 261, 114198.

- Vollertsen, J., Hansen, A.A., 2017. Microplastic in Danish wastewater: Sources, occurrences and fate. The Danish Environmental Protection Agency. Environmental Project.
- Wagner, S., Cattle, S.R., Scholten, T., 2007. Soil-aggregate formation as influenced by clay content and organic-matter amendment. *J. Plant Nutr. Soil Sci.* 170, 173–180.
- Waldschläger, K., Lechthaler, S., Stauch, G., Schüttrumpf, H., 2020. The way of microplastic through the environment—application of the source-pathway-receptor model. *Sci. Total Environ.* 713, 136584.
- Walker, H.W., Bob, M.M., 2001. Stability of particle flocs upon addition of natural organic matter under quiescent conditions. *Water Res.* 35, 875–882.
- Wang, Z., Govers, G., Van Oost, K., Clymans, W., Van den Putte, A., Merckx, R., 2013. Soil organic carbon mobilization by interrill erosion: insights from size fractions. *J. Geophys. Res.* 118, 348–360.
- Weithmann, N., Moller, J.N., Loder, M.G.J., Piehl, S., Laforsch, C., Freitag, R., 2018. Organic fertilizer as a vehicle for the entry of microplastic into the environment. *Sci. Adv.* 4.
- Xu, C.Y., Zhang, B.B., Gu, C.J., Shen, C.S., Yin, S.S., Aamir, M., et al., 2020. Are we underestimating the sources of microplastic pollution in terrestrial environment? *J. Hazard. Mater.* 400.
- Yu, M., van der Ploeg, M., Lwanga, E.H., Yang, X.M., Zhang, S.L., Ma, X.Y., et al., 2019. Leaching of microplastics by preferential flow in earthworm (*Lumbricus terrestris*) burrows. *Environ. Chem.* 16, 31–40.
- Zhang, G., Liu, Y., 2018. The distribution of microplastics in soil aggregate fractions in southwestern China. *Sci. Total Environ.* 642, 12–20.
- Zhou, Y., Wang, J., Zou, M., Jia, Z., Zhou, S., 2020. Microplastics in soils: a review of methods, occurrence, fate, transport, ecological and environmental risks. *Sci. Total Environ.* 748, 141368.
- Zubris, K.A., Richards, B.K., 2005. Synthetic fibers as an indicator of land application of sludge. *Environ. Pollut.* 138, 201–211.